C. R. Chimie 22 (2019) 154–160

Contents lists available at ScienceDirect

Comptes Rendus Chimie

www.sciencedirect.com

Full paper/Mémoire

Modified bentonite for anionic dye removal from aqueous solutions. Adsorbent regeneration by the photo-Fenton process

Selma Khelifi, Fadhila Ayari*

Laboratoire des applications de la chimie aux ressources et substances naturelles et à l'environnement (LACReSNE), Université de Carthage, Faculté des sciences de Bizerte, Zarzouna, 7021, Tunisia

ARTICLE INFO

Article history:
Received 15 July 2018
Accepted 3 December 2018
Available online 17 January 2019

Keywords:
Adsorption
Anionic dye
Photo-Fenton
Regeneration
Bentonite

ABSTRACT

This study aims to present an effective solution for pollutant treatment after adsorption onto modified bentonite. Modified bentonite has been taken as a medium to divide the treatment process of Congo red (CR) dye by a photo-Fenton process into two different processes (separation of CR from wastewater by adsorption and degradation of CR on the surface of the adsorbent by the photo-Fenton process). The adsorbent was characterized by scanning electronic microscopy, zeta potential, and diffuse reflectance spectroscopy techniques. Batch adsorption experiments were carried out to study the effect of the contact time on the adsorption properties of the dye. Kinetics study and isotherm analysis were conducted. The photo-Fenton regeneration of the adsorbent was investigated under different experimental conditions. The results show the success of the regeneration and the total mineralization of the dye.

1. Introduction

The contamination of water by pollutants of various origins is an actual problem [1]. In the textile industries, wastewater is one of the most important sources of pollution of surface waters and groundwater, especially for agricultural land and wildlife [2,3].

The waste products of the textile industries are enormous nuisances for human health and the environment. In fact, the various dyes used cause serious problems because of their stability and low biodegradability [4,5]. Thus, it is necessary to treat these releases before they are discharged into the sewerage system. These effluents contain nonbiodegradable, inhibitory, or toxic substances for most living microorganisms. Moreover, the heterogeneity of their composition makes it difficult or almost impossible to obtain pollution thresholds lower than or equal to those imposed by environmental standards, after treatment by traditional techniques [6,7].

Recent developments in the field of chemical water treatment have led to an improvement in oxidative degradation processes of organic compounds in aqueous media. Oxidation has always been presented as an alternative, with little or no waste and often makes it biodegradable. However, the processes using traditional oxidants (dichloride and its hypochlorous acid derivatives, ozone, dibromide, chlorine dioxide, hydrogen peroxide, potassium permanganate, …) do not completely degrade organic compounds [8]. For this reason, it is essential to look for alternative solutions that solve this problem.

Adsorption has been considered as an attractive method to remove textile dye from aqueous solutions because of its low cost, simplicity, and ease of operation [9]. However, the use of expensive adsorbent can limit the efficiency of this process [10]. In addition, the transfer of the pollutant from the aqueous phase to the solid phase is another source of pollution dangerous for the environment, so it is essential to think of an effective solution that treat the pollutant stored in the solid phase.

* Corresponding author.
E-mail address: fadhilaayari@yahoo.fr (F. Ayari).

https://doi.org/10.1016/j.crci.2018.12.001
1631-0748/

Clay mineral is considered as an alternative material to achieve this point. According to many studies, bentonite clay can improve their properties in several fields [11–14]. For this reason, it is used in this study.

In this study, Tunisian abundant clay, bentonite was prepared and modified via pillaring process using alumina and iron elements to enhance their adsorptive and catalytic properties. The adsorption isotherm and kinetics were determined. Furthermore, the regeneration of this adsorbent was performed through photo-Fenton regeneration.

2. Materials and methods

2.1. Materials and chemicals

2.1.1. Adsorbent preparation

The raw clay used in this study was collected from local deposit sited in the north Tunisia. This clay belongs on smectite family; it was prepared and purified as described in our previous study [15]. It was labeled as Na-Bent.

The modification carried in this bentonite was done via pillaring process by Fe and Al cations. The pillaring process and the most characteristics were reported in our previous study [15]. In this study, we are only interested in Fe-0.1-Pillared Interlayer Clay (PILC) adsorbent, because it has the best adsorbent properties as compared with other adsorbents. Table 1 illustrates the physical characteristics of Na-Bent and Fe-0.1-PILC.

2.1.2. Chemicals

Dye used in this study is the acid diazo dye Congo red (FW = 676.66), noted CR. The chemical structure of this dye contains an azochromophore group (−N═N) and an auxochromic acid group ($-SO_3H$) associated with the benzene structure.

For an aqueous solution of concentration 10^{-4} mol L^{-1}, at a natural pH (pH = 7), the absorption spectrum of this dye in the ultraviolet–visible (UV–vis) region is represented in Fig. 1. The CR has a main band at 497 nm, attributed to the absorption band of the anionic monomer and associated with an absorption band in the UV region at λ = 347 nm, attributed to the naphthalene group.

All chemicals used in this study were of analytical grade and used without further purification.

2.2. Adsorption and photo-Fenton regeneration experiments

2.2.1. Adsorption experiments

For this experiment, 0.1 g of FeAl-PILC adsorbent was placed in a 100 mL Erlenmeyer flask containing 50 mL of dye solution at desired concentration.

Table 1
Specific surface, pore volume, and CEC of studied samples. CEC: Cationic Exchange Capacity

Samples	S_{BET} ($m^2\ g^{-1}$)	S_{mp} ($m^2\ g^{-1}$)	V_{mp} ($cm^3\ g^{-1}$)	V_{PT} ($cm^3\ g^{-1}$)	CEC (mequiv/100 g)
Na-Bent	72.2	16.06	0.008	0.07	89
Fe-0.1-PILC	50.09	0	0	0.05	17.33

CEC: Cationic Exchange Capacity

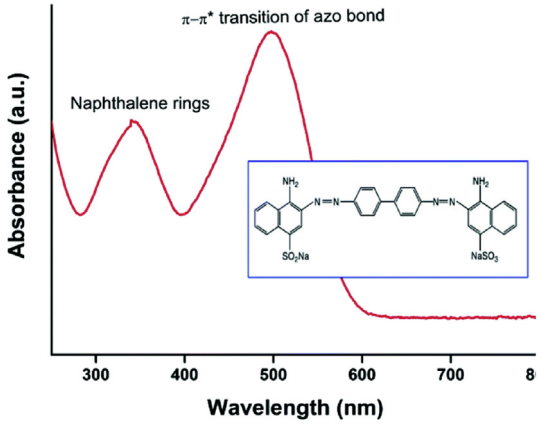

Fig. 1. UV–vis spectra of CR dye at pH = 7.

For kinetics studies of CR adsorption, 2–3 mL of the solution was collected at various time intervals with a syringe. The adsorbent was separated from the liquid phase by centrifugation at 3000 rpm for 20 min and filtered through a 0.45 μm filter. Then, the dye remained in the solution was determined using a UV–vis spectrophotometer (Shimadzu Model PerkinElmer). Absorbance measurements were made at the maximum wavelength of CR at 498 nm in neutral medium.

The percentage of CR adsorption (% Adsorption) and the amount of CR adsorbed (Q_{ads}) were calculated by the following relations, respectively:

$$\%\ \text{Adsorption} = \frac{(C_0 - C_e)}{C_0} \times 100 \quad (1)$$

$$Q_{ads} = \frac{(C_0 - C_e) \times V}{m} \quad (2)$$

where C_0 and C_e are the initial and equilibrium concentrations of CR (mg L^{-1}), respectively. V is the volume of the dye solution (L) and m is the mass of adsorbent (g).

2.2.2. Photo-Fenton experiments

The photocatalytic regeneration of desired amounts of as-synthesized microporous materials was assessed by the photodegradation of 150 mL CR aqueous solution (with 5×10^{-4} M concentration at natural pH). The suspension was set aside with magnetic stirring at room temperature and dark conditions for desired time to reach the adsorption–desorption equilibrium for FeAl-PILC. After that, the required amount of H_2O_2 was added and the suspension was exposed to UV light irradiations for desired time (0–120 min). During reaction, 3 mL of the suspension was taken for analysis, centrifuged to remove the adsorbent, and filtered through a 0.45-μm filter membrane.

The calculation of CR degradation was performed, taking into account the initial adsorption on the material surface (Eq. 3):

$$\%\ \text{Degradation} = (C_0 - C_t)/C_0 \times 100 \quad (3)$$

where C_t is the CR concentration at time t (min) and C_0 is

the initial concentration after stabilization because of the adsorption on the adsorbent surface.

2.3. Analysis and instruments

The morphology and surface of Na-Bent and Fe-0.1-PILC were examined with scanning electronic microscopy (SEM, Hitachi SU-70; at the acceleration voltage 15 kV) coupled with Energy Dispersive X-ray (EDX) microanalyzer (PGT IMIX PC) to evaluate the chemical composition.

The values of zeta potential were measured using a Malvern zeta meter (Zetasizer). These values were determined through adjusting pH from 2 to 9 by adding HCl (0.1 M) or NaOH (0.1 M) at 25 °C. UV–vis diffuse reflectance spectra were measured using a UV–vis spectrophotometer (PerkinElmer, Lambada 950).

3. Results and discussion

3.1. Material properties

Additional techniques SEM, diffuse reflectance spectroscopy (DRS), and zeta potential were applied to characterize the prepared AlFe-PILC sample.

The SEM micrographs of natural and Fe-0.1-PILC are presented in Fig. 2. SEM images are fundamental to clarify the changes in the morphological surface upon Al and Fe pillaring. As can be seen, the surface morphology of natural clay Na-Bent (Fig. 2(a)) is different as compared with Fe-0.1-PILC (Fig. 2(b)).

The EDX spectrum presented in Fig. 2 indicates the increase in Al and Fe amounts after the pillaring process. Also, the existence of certain elements, such as Si, Na, K, and Mg, which are constituents of starting bentonite, can be seen.

pH_{pzc} is the pH at which the electrical charge density on solid surface is zero. As can be known, adsorption of a dye molecule onto the solid surface is so influenced by pH_{pzc}. Hence, at higher pH than pH_{pzc}, adsorbent surface is negatively charged and attracts cations. Conversely, below pH_{pzc}, the catalyst surface is positively charged and repels cations [16]. The zero point charge of our synthesized materials was found to be 5.4 for Na-Bent and 3 for Fe-0.1-PILC (see Fig. 3).

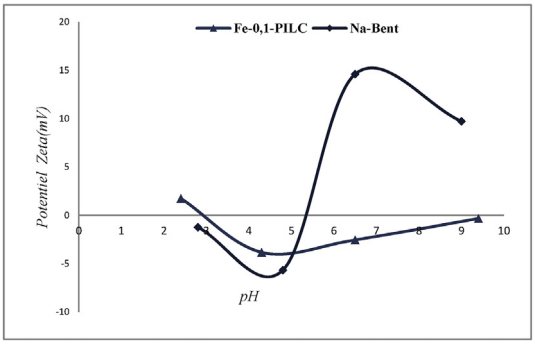

Fig. 3. Zeta potential of Na-Bent and pillared bentonites Fe-0.1-PILC.

The optical properties of the studied adsorbents were investigated with UV–vis DRS using a UV–vis spectrophotometer (Shimadzu UV-2700). As shown in Fig. 4, the Na-Bent presented UV light absorption only, whereas the synthesized FeAl-Bent exhibited adsorption in the visible light region. The UV–vis DRS results indicated that the optical responses of bentonite could be extended to the visible light region after intercalation by Fe and Al polycations. The visible light energy could be used by FeAl-Bents for realizing the photoelectric effects.

3.2. Adsorption of CR on Na-Bent and Fe-0.1-PILC

The influence of stirring time on the CR adsorption is an important step leading to determine the time necessary to establish the equilibrium adsorption–desorption. This study was conducted on Na-Bent and Fe-0.1-PILC in batch mode.

This involves introducing 100 mL of CR solution with 0.1 g of the adsorbent, for 100 min, at room temperature (25 °C), at natural pH and under continuous stirring. According to the literature, 60 min is sufficient to establish the adsorption–desorption equilibrium for clays [17,18]. Obtained results are shown in Fig. 5.

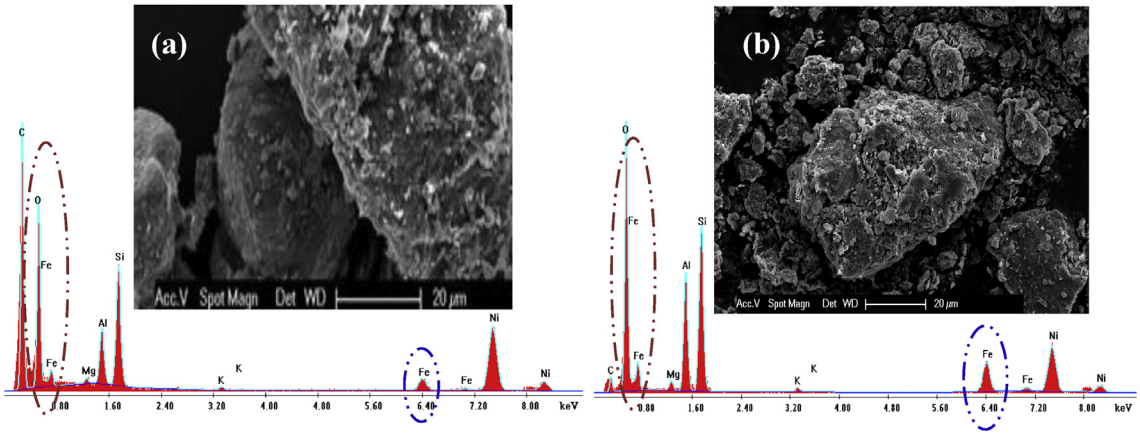

Fig. 2. SEM micrographs of Na-Bent (a) and Fe-0.1-PILC (b).

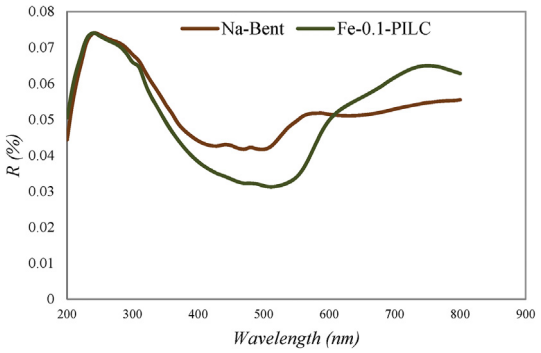

Fig. 4. UV–vis diffuse reflectance spectrum of Na-Bent and Fe-0.1-PILC.

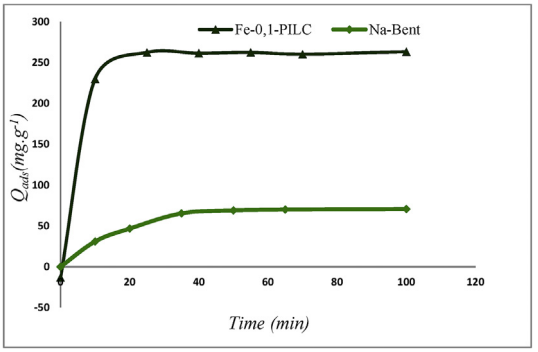

Fig. 5. Adsorption kinetics of CR onto Fe-0.1-PILC and Na-Bent ([CR] = 5×10^{-4} mol L^{-1}, $m_{adsorbant}$ = 0.1 g, T = 25 °C, and pH = 7).

From Fig. 5, it is noted that CR adsorption on Fe-0.1-PILC appears to be rapid, the equilibrium is reached before 20 min of contact but it is slow with Na-Bent, the saturation time is 40 min with this clay.

For Fe-0.1-PILC, the adsorption rate of CR is reached 70% for an initial concentration of 5×10^{-4} mol L^{-1}. However, it does not exceed 29% for Na-Bent. This shows the enhancement of the adsorptive capacity of the purified clay after modification with iron and alumina polycations. These results are deduced, thanks to the textural and structural properties of Fe-0.1-PILC even the large basal spacing that favors the adsorption phenomenon. This is in agreement with the previous study [19].

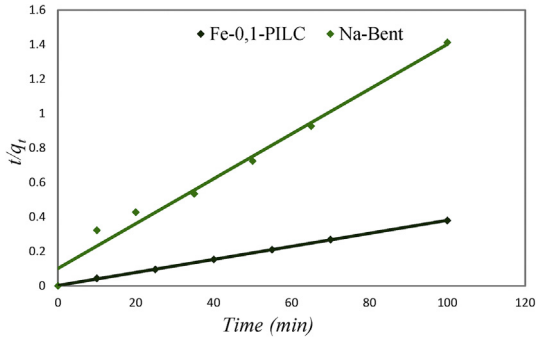

Fig. 6. Pseudo-second-order kinetic model of Fe-0.1-PILC and Na-Bent.

To better understand the mechanism that governs the adsorption phenomenon of these adsorbents, a kinetic modeling is made to the results of this study. Then, Fig. 6 represents the pseudo-second-order model adsorption of CR on Fe-0.1-PILC and Na-Bent. Thus, kinetic parameters and correlation coefficients are illustrated in Table 2.

The pseudo-second-order model well describes the experimental results of CR adsorption on the purified and pillared clay according to the values of the correlation coefficients, which are closer to unity. This suggests that the adsorption mechanism is based on physisorption [18,20]. Chen and Zhao [21] reported the same results for organo-attapulgite adsorption of CR by showing that pseudo-second-order model is the most appropriate model and that physisorption is the main mechanism that controls the speed of the adsorption process.

3.2.1. Adsorption isotherm

To evaluate the maximum adsorption capacity of CR adsorbed on the adsorbents, a study of the adsorption isotherms was carried out. The amount of CR adsorbed (Q_{ads}) as a function of its equilibrium concentration (C_e) was obtained at pH = 7 and at 25 °C, for CR solutions at concentrations ranging from 10^{-5} to 10^{-3} mol L^{-1}, mixed with Na-Bent and Fe-0.1-PILC at 0.1 g. Fig. 7 shows the adsorption isotherms obtained.

According to the classification of Giles et al. [22], the adsorption isotherm of the CR by the modified clay (Fe-0.1-PILC) is of type H reflecting a relatively high affinity of the solid phase for the adsorbed substance. This isotherm indicates a significant adsorption of the dye with an adsorption rate of 80% and fast kinetics.

When the adsorbent is Na-Bent, the adsorption isotherm is of S type and is divided into two stages:

- the first one is characterized by a weak adsorption where the dye is probably retained by the electrostatic forces;
- the second step is characterized by a remarkable variation in the adsorption showing that the matrix involves strong interactions both between adsorbent and adsorbate and between the CR molecules themselves.

Two models are introduced to analyze the experimental data of the adsorption isotherms: Langmuir and Freundlich models.

Fig. 8(a) and (b) illustrates the modeling results of these two models and the main specific parameters of each model are summarized in Table 2.

The Langmuir model is applicable for the modeling of the experimental results obtained by Fe-0.1-PILC according to the value of the correlation coefficient ($R^2 \approx 1$). This finding implies that the equilibrium data correspond to the Langmuir model and the adsorption process is mainly monolayer [23,24]. The value of $Q_{max,cal}$ inferred from the slope of this straight line is 500 mg g^{-1}, which is very close to the experimental value $Q_{max,exp}$ = 451 mg g^{-1}.

The separation factor R_L is known as a dimensionless parameter that judges the possibility of sorption. Its value

Table 2
Kinetics modeling parameters.

Kinetic modeling								
	Pseudo first order			*Pseudo second order*				
	Q_e	K_1	R^2	Q_e	K_2	R^2		
Na-Bent	35.02	0.032	0.902	76.92	0.0018	0.980		
Fe-0.1-PILC	133.8	0.0047	0.455	333.33	0.0012	0.998		
Isotherm modeling								
	Freundlich			*Langmuir*				
	K_F	n	R^2	$Q_{max,cal}$ (mg g^{-1})	$Q_{max,exp}$ (mg g^{-1})	K_L (L mg^{-1})	R_L	R^2
Na-Bent	0.132	0.76	0.961		–	–	1.148	0.385
Fe-0.1-PILC	46.29	2.347	0.868	451	500	13	0.987	0.982

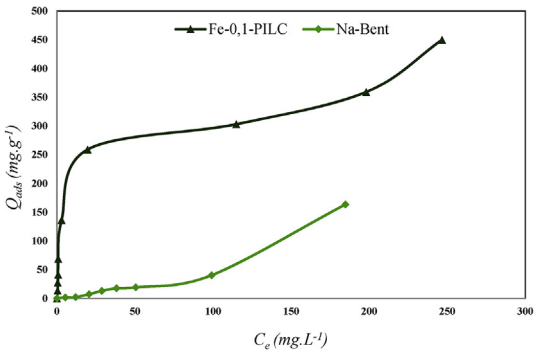

Fig. 7. Adsorption isotherm of CR onto Fe-0.1-PILC and Na-Bent (m_{ads} = 0.1 g, pH = 7, and T = 25 °C).

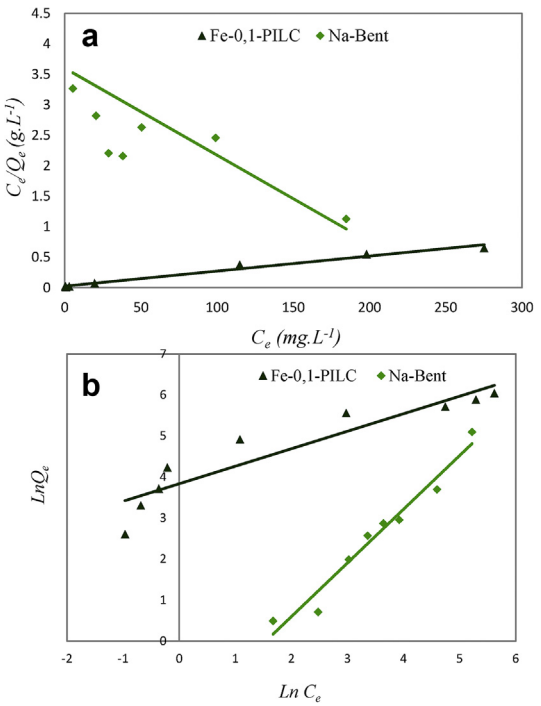

Fig. 8. Adsorption isotherm of CR by Na-Bent and Fe-0.1-PILC according to the Langmuir (a) and Freundlich (b) models.

of 0.987 suggests that the Langmuir model is favorable [25,26].

For Na-Bent, a better correlation of the results was obtained using the Freundlich model, confirmed by a correlation coefficient R^2 close to unity that could explain a continuous distribution of the adsorption sites.

3.3. Photo-Fenton regeneration of Fe-0.1-PILC

Photocatalytic regeneration of Fe-0.1-PILC saturated on CR was evaluated as follow: 0.1 g of Fe-0.1-PILC was added to 150 mL of dye solution with a concentration of 5 × 10^{-4} mol L^{-1} at preferred pH. Each reaction mixture (catalyst + CR solution) was stirred in the dark for 40 min to reach the adsorption–desorption equilibrium of dye onto the adsorbent surface. After that, a desired amount of H_2O_2 was added and the lamp was turned on.

Fig. 9 shows the regeneration of adsorbent by different ways: under UV light irradiations only, the percentage degradation was 15.6% after 120 min. In the dark condition and in the presence of H_2O_2 (Fenton process), a maximal CR degradation is 51.38%, whereas it exhibited a prominent degradation efficiency with photo-Fenton process; percentage degradation reaches 98%.

3.3.1. Factors influencing adsorbent regeneration

In this section, H_2O_2 concentration and pH were investigated, respectively, to understand their effects on the adsorbent regeneration and the results are given in Fig. 10.

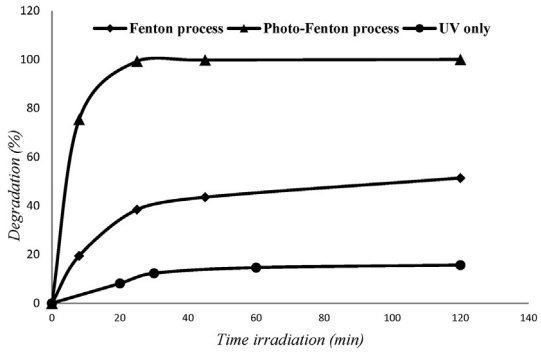

Fig. 9. Adsorbent regeneration via different ways.

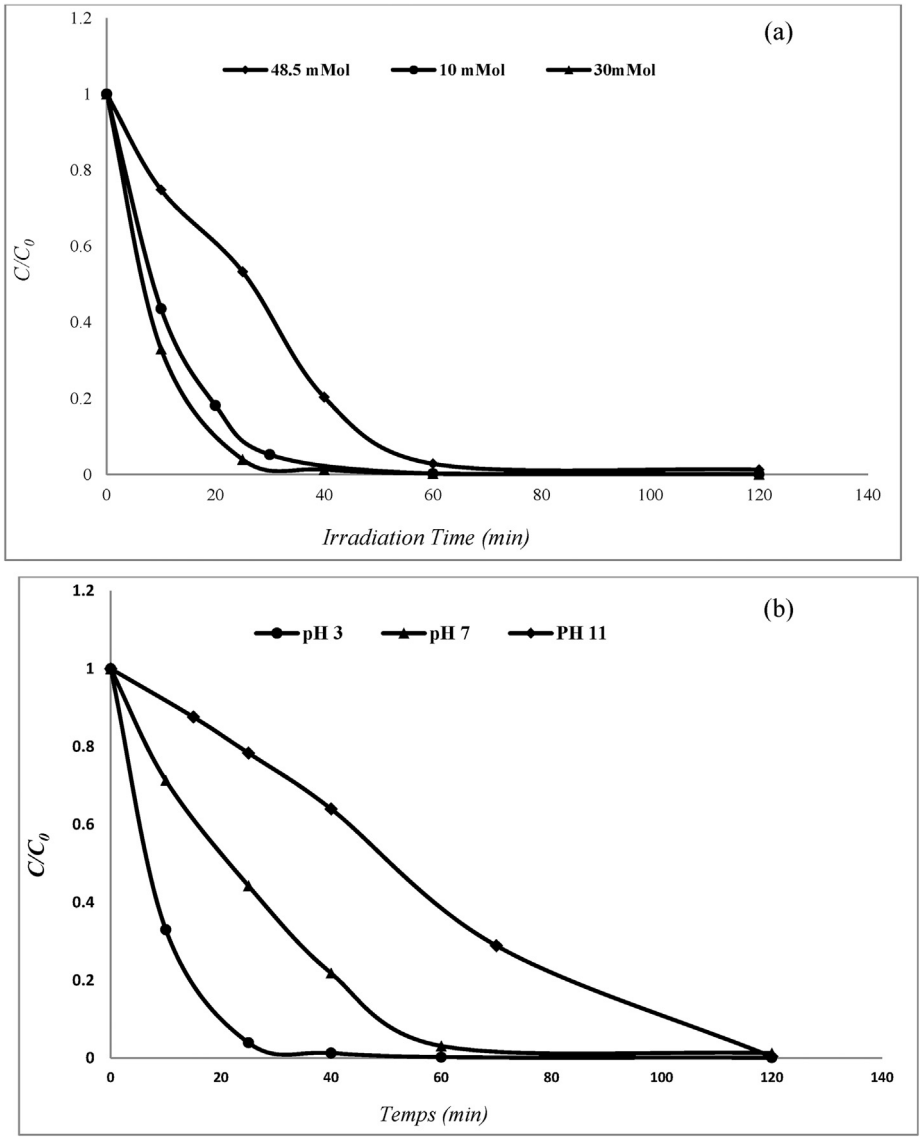

Fig. 10. Effect of H_2O_2 concentration (a) and pH (b) on the Fe-0.1-PILC regeneration (adsorbent dose = 0.1 g [CR] = 5×10^{-4} mol L^{-1}, and $T = 25$ °C).

The regeneration of Fe-0.1-PILC by the photo-Fenton process is based on the interaction of hydroxyl radicals HO• with CR dye adsorbed on the adsorbent surface. Thus, the dosage of H_2O_2 (oxidant) and Fe-0.1-PILC is very important for the process of regeneration. The oxidation of CR by H_2O_2 is given as shown in chemical reaction (4):

$$C_{32}H_{22}N_6Na_2O_6S_2 + 91\,H_2O_2 \rightarrow 32\,CO_2 + 98\,H_2O + 6\,NO_3^- + 2\,SO_4^{2-} + 2\,Na^+ + 8\,H^+ \quad (4)$$

According to this chemical reaction, it can be seen that theoretical amount of H_2O_2 for completely oxidizing 1 mol CR is 91 mol of H_2O_2. In this study, 10, 30, and 48.5 mmol L^{-1} H_2O_2 was selected for studying the effect of H_2O_2 concentration (Fig. 10(a)). It can be noted that Fe-0.1-PILC can be regenerated with the increase in H_2O_2 concentration, the degradation percentage increases rapidly until H_2O_2 reaches to 30 mmol L^{-1}. Additional increase in H_2O_2 dosage results in the decrease of percentage degradation. This can be explained as follows: a higher H_2O_2 dosage can increase the production rate of $HO^{\bullet}$, resulting in the increase of percentage degradation. However, the excessive amount of H_2O_2 can increase the possibility of secondary reactions between H_2O_2 and HO (reactions (5) and (6)), resulting in the decrease of effective activity of $HO^{\bullet}$ [27].

$$H_2O_2 + HO^{\bullet} \rightarrow H_2O + HO_2^{\bullet} \quad (5)$$

$$HO^{\bullet} + HO^{\bullet} \rightarrow H_2O_2 \quad (6)$$

The effect of pH was investigated at three pH values 3, 7, and 11. It can be seen from Fig. 10(b) that pH = 3 is the optimal value for the adsorbent regeneration. With the increase in pH, the percentage degradation decreases.

Therefore, the mechanism of the regeneration associated with the heterogeneous photo-Fenton process would be described as follows:

- the molecules of CR dye on the adsorbent surface absorbed the photons from UV light to generate excited states (reaction (7));
- the generation of Fe(II) species resulted after the reaction between excited dye and Fe(III) species (reaction (8));
- the reaction between Fe(II) generated and H_2O_2 took place producing HO radicals (reaction (9));
- the initiation of the degradation of the adsorbed dye and the regeneration of Fe-0.1-PILC (reaction (10)),

$$\equiv\text{Dye} + \text{UV light} \rightarrow \equiv\text{Dye}^{*} \quad (7)$$

$$\equiv\text{Dye}^{*} + \equiv\text{Fe(III)} \rightarrow \equiv\text{Fe(II)} + \equiv\text{Dye}^{+\cdot} \quad (8)$$

$$\equiv\text{Fe(II)} + H_2O_2 \rightarrow \equiv\text{Fe(III)} + HO^{\cdot} + HO^{-} \quad (9)$$

$$HO^{\cdot} + \equiv\text{Dye}/\equiv\text{Dye}^{+\cdot} \rightarrow NO_3^{-} + SO_4^{2-} + CO_2 + H_2O \quad (10)$$

where the symbol ≡ represents the iron species or the dye on the solid.

To analyze the degradation products formed during the regeneration of Fe-0.1-PILC by photo-Fenton process, the ionic chromatography (Dionex DX-500) analysis was done for the quantification of inorganic ions NO_3^- and SO_4^{2-}. Result shows a total mineralization of CR to SO_4^{2-}, which confirms the regeneration of adsorbent.

4. Conclusions

Adsorption of CR by bentonite and pillared bentonite Fe-0.1-PILC was studied and appreciable results were reported. Adsorptive capacity of Na-Bent is enhanced remarkably after modification and obtained results indicate that pillared bentonite can be an efficient adsorbent for the anionic dye. The photo-Fenton process can be applied to regenerate this adsorbent through the total degradation of dye adsorbed. So, according to obtained results in this study, it is very important to conclude that the problem of the safe disposal of the contaminated solids can be effectively resolved. In addition, the use of natural abundant material and UV light lamps can reduce the cost of starting materials and experimental process. The combination of adsorption on modified bentonite and the efficient photo-Fenton regeneration would be an approach for the destruction of pollutants in water.

References

[1] G. Ghasemzadeh, M. Momenpour, F. Omidi, M.R. Hosseini, M. Ahani, A. Barzegari, Front. Environ. Sci. Eng. 8 (4) (2014) 471–482.
[2] H. Chaker, L. Chérif-Aouali, S. Khaoulani, A. Bengueddach, S. Fourmentin, J. Photochem. Photobiol. Chem. 318 (2016) 142–149.
[3] J.R. Guimarães, M.G. Maniero, R.N. de Araújo, J. Environ. Manag. 110 (2012) 33–39.
[4] H. Hou, R. Zhou, P. Wu, L. Wu, Chem. Eng. J. 211 (2012) 336–342.
[5] C. Sudipta, D.S. Lee, M.W. Lee, S.H. Woo, Bioresour. Technol. 100 (11) (2009) 2803–2809.
[6] M. Tekbaş, H.C. Yatmaz, N. Bektaş, Microporous Mesoporous Mater. 115 (3) (2008) 594–602.
[7] L. Cottet, C.A.P. Almeida, N. Naidek, M.F. Viante, M.C. Lopes, N.A. Debacher, Appl. Clay Sci. 95 (2014) 25–31.
[8] J.N. Tiwari, K. Mahesh, N.H. Le, K.C. Kemp, R. Timilsina, R.N. Tiwari, K.S. Kim, Carbon 56 (2013) 173–182.
[9] C. Srilakshmi, R. Saraf, Microporous Mesoporous Mater. 219 (2016) 134–144.
[10] S. Lin, Z. Song, G. Che, A. Ren, P. Li, C. Liu, J. Zhang, Microporous Mesoporous Mater. 193 (2014) 27–34.
[11] J. Feng, X. Hu, P.L. Yue, Environ. Sci. Technol. 38 (1) (2004) 269–275.
[12] A.M. Elfadly, I.F. Zeid, F.Z. Yehia, M.M. Abouelela, A.M. Rabie, Fuel Process. Technol. 163 (2017) 1–7.
[13] D.S. Moraes, R.S. Angélica, C.E.F. Costa, G.N. Rocha Filho, J.R. Zamian, Appl. Clay Sci. 51 (3) (2011) 209–213.
[14] V.A. Cardozo, R. Sánchez-Obregón, H. Salgado-Zamora, R. Jiménez-Juárez, Monatsh. Chem. 146 (8) (2015) 1335–1337.
[15] S. Khelifi, F. Ayari, A. Choukchou-Braham, D. Ben HassenChehimi, J. Porous Mater. 25 (3) (2018) 885–896.
[16] H. BelHadjltaief, M. Ben Zina, M.E. Galvez, P. Da Costa, J. Photochem. Photobiol. A: Chem. 315 (2016) 25–33.
[17] F. Ayari, S. Khelifi, M. Trabelsi-Ayadi, Environ. Technol. (2018) 1–31.
[18] F. Ayari, S. Mezghuich, A. Ben Othmen, M. Trabelsi-Ayadi, Desalin. Water Treat. 105 (2018) 332–342.
[19] T. Undabeytia, M.C. Galán-Jiménez, E. Gómez-Pantoja, J. Vázquez, B. Casal, F. Bergaya, E. Morillo, Appl. Clay Sci. 80 (2013) 382–389.
[20] Y.-S. Ho, G. McKay, Process Biochem. Process Biochem. 34 (1999) 451–465.
[21] H. Chen, J. Zhao, Adsorption 15 (2009) 381–389.
[22] C.H. Giles, T. MacEwan, S. Nakhwa, D. Smith, J. Chem. Soc. 786 (1960) 3973–3993.
[23] F. Ayari, Nanotechnology for Sustainable Water Resources, Wiley Online Library, 2018, pp. 407–459.
[24] M. Zhang, Q. Yao, C. Lu, Z. Li, W. Wang, ACS Appl. Mater. Interfaces 6 (2014) 20225–20233.
[25] F. Ayari, E. Srasra, M. Trabelsi-Ayadi, Desalination 206 (2007) 270–278.
[26] S. Bentahar, A. Dbik, M. El Khomri, N. El Messaoudi, A. Lacherai, Groundwater Sustain. Dev. 6 (2018) 255–262.
[27] L. Wang, J. Zhang, R. Zhao, C. Li, Y. Li, C. Zhang, Desalination 254 (2010) 68–74.